Acta Pharmaceutica Sinica B 2021;11(5):1261−1273

Chinese Pharmaceutical Association
Institute of Materia Medica, Chinese Academy of Medical Sciences

Acta Pharmaceutica Sinica B

www.elsevier.com/locate/apsb
www.sciencedirect.com

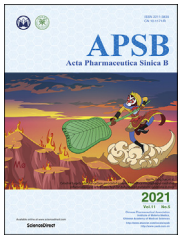

ORIGINAL ARTICLE

SMYD3−PARP16 axis accelerates unfolded protein response and mediates neointima formation

Fen Long[a], Di Yang[a], Jinghua Wang[a], Qing Wang[a], Ting Ni[b], Gang Wei[b], Yizhun Zhu[c,*], Xinhua Liu[a,*]

[a]*Pharmacophenomics Laboratory, Human Phenome Institute, Fudan University, Shanghai 201203, China*
[b]*State Key Laboratory of Genetic Engineering & MOE Key Laboratory of Contemporary Anthropology, Collaborative Innovation Center of Genetics and Development, School of Life Sciences and Shanghai Cancer Center, Fudan University, Shanghai 200438, China*
[c]*State Key Laboratory of Quality Research in Chinese Medicine and School of Pharmacy, Macau University of Science and Technology, Macau, China*

Received 8 July 2020; received in revised form 24 August 2020; accepted 13 October 2020

KEY WORDS

PARP16;
Neointimal hyperplasia;
Vascular smooth muscle cell;
Endoplasmic reticulum;
SMYD3

Abstract Neointimal hyperplasia after vascular injury is a representative complication of restenosis. Endoplasmic reticulum (ER) stress-induced unfolded protein response (UPR) is involved in the pathogenesis of vascular intimal hyperplasia. PARP16, a member of the poly(ADP-ribose) polymerases family, is correlated with the nuclear envelope and the ER. Here, we found that PERK and IRE1α are ADP-ribosylated by PARP16, and this might promote proliferation and migration of smooth muscle cells (SMCs) during the platelet-derived growth factor (PDGF)-BB stimulating. Using chromatin immunoprecipitation coupled with deep sequencing (ChIP-seq) analysis, PARP16 was identified as a novel target gene for histone H3 lysine 4 (H3K4) methyltransferase SMYD3, and SMYD3 could bind to the promoter of *Parp16* and increased H3K4me3 level to activate its host gene's transcription, which causes UPR activation and SMC proliferation. Moreover, knockdown either of PARP16 or SMYD3 impeded the ER stress

Abbreviations: ATF6, activating transcription factor 6; BIP, immunoglobulin heavy-chain binding protein; DAPI, 4′,6-diamidino-2-phenylindole; EGCG, epigallocatechin-3-gallate; ER, endoplasmic reticulum; UPR, unfolded protein response; ECM, extracellular matrix; H3K4, histone H3 lysine 4; IRE1, inositol-requiring enzyme 1; MMP, matrix metal proteinase; PDGF, platelet-derived growth factor; PARP, poly(ADP-ribose) polymerases; PERK, protein kinase R (PKR)-like ER kinase; p-PERK, phosphate-PKR-like ER kinase; p-eIF2α, phosphate-eukaryotic initiation factor 2α; PCNA, proliferating cell nuclear antigen; SMYD3, SET and MYND domain containing 3; SMCs, smooth muscle cells; VSMCs, vascular smooth muscle cells; VCAM-1, vascular cell adhesion molecule-1; XBP-1, X-box binding protein-1; siRNA, small interfering RNA; ChIP-seq, chromatin immunoprecipitation coupled with deep sequencing; IACUC, Institutional Animal Care and Use Committee.

*Corresponding authors. Tel.: +86 21 51980159, +853 8879 2880; fax: +853 2882 7222.
E-mail addresses: yzzhu@must.edu.mo (Yizhun Zhu), liuxinhua@fudan.edu.cn (Xinhua Liu).

Peer review under responsibility of Institute of Materia Medica, Chinese Academy of Medical Sciences and Chinese Pharmaceutical Association.

https://doi.org/10.1016/j.apsb.2020.12.010

and SMC proliferation. On the contrary, overexpression of PARP16 induced ER stress and SMC proliferation and migration. *In vivo* depletion of PARP16 attenuated injury-induced neointimal hyperplasia by mediating UPR activation and neointimal SMC proliferation. This study identified SMYD3−PARP16 is a novel signal axis in regulating UPR and neointimal hyperplasia, and targeting this axis has implications in preventing neointimal hyperplasia related diseases.

1. Introduction

Intimal hyperplasia, as representative complication of restenosis and atherosclerotic plaques, is the thickening of a blood vessel wall in response to injury[1,2]. It is also widely recognized that proliferation, migration and inflammatory phenotypic switching of vascular smooth muscle cells (VSMCs) are the significant basis for intimal hyperplasia[3,4]. In response to vessel injury, VSMCs dedifferentiate and aggressively proliferate and migrate to the vessel lumen, where they secrete extracellular matrix (ECM) and form a neointima[5]. Although preventive intervention with drug-eluting stent exerts an inhibitory effect on neointimal hyperplasia, those drugs also cause higher cardiac risk and deferred vessel function[6]. Consequently, understanding the complex mechanisms and finding effective strategies to ameliorate neointimal hyperplasia have essential clinical significance.

Endoplasmic reticulum (ER) stress is a fundamental cellular response, and subsequently results in activation of unfolded protein response (UPR) comprising three sensors/effectors of ER protein misfolding; PERK (protein kinase R [PKR]-like ER kinase), IRE1 (inositol-requiring enzyme 1), and ATF6 (activating transcription factor 6)[7,8]. Severe or prolonged perturbed ER homeostasis or ER stress will ultimately lead to proliferation and inflammatory status of VSMCs, which contributes significantly to the development and progression of vascular remodeling[9−11]. It has been proven that ER stress promotes the neointimal formation, and alleviation of ER stress inhibits neointimal hyperplasia in a wire-induced vascular injury model[12]. Accordingly, inhibition of ER stress is a putative strategy for treating cardiovascular diseases[13]. The poly(ADP-ribose) polymerases (PARPs) are consisted of at least 18 members, PARP16 is the only known member as a tail-anchored protein with putative C-terminal transmembrane tract correlated with the nuclear envelope and the ER[14]. It was reported that ADP-ribosylation modification of PERK and IRE1α by PARP16 is required for PERK and IRE1α activation during the UPR[15]. However, whether PARP16 mediating neointima formation through promoting UPR remains unclear.

Several pieces of evidence suggest that histone modification enzymes play a role in regulating of gene expression, SET and MYND domain-containing protein 3 (SMYD3) is a lysine methyltransferase and can catalyze trimethylation of lysine 4 at histone 3 (H3K4), which predominantly associates with active promoters[16,17], to induce genes involved in cell cycle and transcription regulation[18,19]. Besides its H3K4me3-dependent function, SMYD3 also modifies non-histone proteins to regulate specific cellular reactions[20]. However, it remains unclear whether SMYD3 regulates PARP16 gene transcription, which affects ER stress and intimal hyperplasia.

Here, to evaluate PARP16 on neointimal hyperplasia, we assessed its effect on the proliferation and migration of VSMCs *in vitro* and neointima formation following ligation or balloon-induced vascular injury. Strikingly, we found that PARP16 ablation resulted in inhibition of intimal hyperplasia through mediating ER stress and disrupting VSMCs proliferation and migration. Moreover, *Parp16* was identified as a potential target gene of SMYD3 by mediating methylation status of H3K4 in the promoter. Our findings provided insight into the role of SMYD3-mediated PARP16 on neointimal hyperplasia following arterial injury, offering a potential therapeutic target for vascular diseases.

2. Materials and methods

2.1. Chemicals and materials

Reagent sources were as follows: platelet derived growth factor (PDGF)-BB was purchased from Sigma−Aldrich (GF-149, St. Louis, MO, USA). Epigallocatechin-3-gallate (EGCG, MB1672), brefeldin A (BFA, MB3357), and tauroursodeoxycholic acid (TUDCA, MB5423) were purchased from Meilun Biotechnology (Dalian, China). EPZ031686 (HY-19324) was purchased from MCE (MedChemExpress, USA). Antibodies were obtained from the following sources: PARP16 (ARP33751) was purchased from Aviva Systems Biology Corp. (San Diego, CA, USA); matrix metalloproteinase 9 (MMP9, sc-393,859) was purchased from Santa Cruz Biotechnology (Santa Cruz, CA, USA); p-PERK (3191), p-eIF2α (3398) and H3K4me3 (9751) were purchased from Cell Signaling Biotechnology (Danvers, MA, USA); proliferating cell nuclear antigen (PCNA, ab92552), cyclin E (ab71535), cyclin D1 (ab134175), PARP16 (ab154510), ATF6 (ab11909), and XBP1 (ab37152) were purchased from Abcam (Cambridge, UK); vascular cell adhesion molecule-1 (VCAM-1, GTX12133) was obtained from GeneTex (CA, USA); p-IRE1α (AP0878) was purchased from ABclonal (Wuhan, China); BIP (11587-1-AP), collagen III (22734-1-AP), GAPDH (60004-1-Ig), calnexin (10427-2-AP), SMYD3 (12011-1-AP) and DDDK tag (Flag, 66008-3-Ig) were purchased from Proteintech (USA). Anti-mono- and poly-ADP-ribose binding reagent (MABE1075) was obtained from Merck (Merck Millipore, USA).

2.2. Rat vascular smooth muscle cell (rVSMC) isolation and culture

rVSMCs were isolated from the thoracic aortic arteries of rats based on previous description[21]. The isolated rVSMCs were

cultured using the Dulbecco's modified Eagle's medium containing 10% fetal bovine serum (FBS, HyClone).

Human vascular smooth muscle cell (hVSMC) was obtained from ScienCell and cultured in SMC medium, with an addition of 1% smooth muscle cell growth supplement and 2% FBS (ScienCell, USA). The cells on passages 3−7 were used for the experiments.

2.3. Western blot

The total protein collected from cells and vascular tissues were separated *via* SDS-PAGE and then transferred to membranes. After blocked in 5% non-fat milk, the membranes were incubated with primary antibody followed by IRDye 800 C W secondary antibody (LI-COR Biotechnology, Nebraska, USA). The proteins were visualized by Odyssey infrared imaging system and quantified for relative expression levels by Alpha Imager (Alpha Innotech Corp, San Leandro, CA, USA).

2.4. Real-time quantitative polymerase chain reaction (RT-qPCR)

Total RNA of VSMCs and tissues was isolated with Trizol, reverse transcribed, and subjected to real-time PCR. Primer sequences of gene are as follows (Forward, Reverse):

Parp16: 5′-CTCCTTGGCCAGACCCTTAG-3′, 5′-GATAGAGGGACATCGCGACC-3′;

Bip: 5′-AGTTGTGACTGTACCAGCTTACT-3′, 5′-ACATCGAAGGTTCCACCACC-3′;

Grp94: 5′-GGACATGCTGCGGAGGGTTA-3′, 5′-CTGAGGCGGAGCATCCTTTC-3′;

Chop: 5′-GCTTGCTGAAGAGAACGAGC-3′, 5′-GACTGACCATGCGGTCGAT-3′;

Pdi: 5′-GGTGGACTCAAGCGAAGTGA-3′, 5′-GGTGGACTCAAGCGAAGTGA-3′;

Atf4: 5′-CTGAGTCCTACCTGGGCTCT-3′, 5′-TTTGGGTCGAGAACCACGAG-3′.

Level of expression was quantified by $2^{-\Delta\Delta C_t}$ equation, with *Gapdh* as control for normalization.

2.5. Small interfering RNA transfection

Rat *Parp16* small interfering RNA (siRNA), human *PARP16* siRNA, rat *Smyd3* siRNA and control siRNA were produced by GenePharma (Shanghai, China). Sequences corresponding to the siRNA of were as follows:

Rat *Parp16*: 5′-CCUACCUCACAAGUGACUUTT-3′;

Rat *Smyd3*: 5′-CUGAUGCGGUGUUCUCAAUTT-3′;

Human *PARP16*: 5′-CCUCAAAGGUCCUGACAAUTT-3′, 5′-CCAUUCCAUUAUCCACAAUTT-3′, and 5′-GCAGACGAGCGAGAAUCAATT-3′. Transfection of siRNA was carried using Lipofectamine RNAiMAX (13,778,150, Thermo Fisher Scientific, USA) based on the manufacturer's instructions. For *in vivo* studies, 15 μg of the siRNA dissolved in 30% Poloxamer solution was perivascularly delivered to the rat carotid arteries immediately after injury as previously described. A control siRNA was applied as a negative control.

2.6. Lentivirus generation and infection

For construction of lentiviral-mediated over-express rat PARP16, the *Parp16* cDNA was amplified from rat genomic DNA and then cloned into the vector pCDH-CMV-MCS-EF1-copGFP. The construct was confirmed by DNA sequencing. Sequences of primers were as follows: 5′-CCGGAATTCATGCAGCTCTCCAACAGGG-3′, and 5′-CGCGGATCCTCTCTTCAGGCGATTCCAG-3′. The human Flag-PARP16 plasmid and the negative control vector were made by Hanbio (Shanghai, China).

To obtain the lentivirus, the recombinant plasmid and packaging vectors pMD2.0G and psPAX2 were co-transfected into HEK293T cells using the transfection reagent lipofectamine 2000 (11668019, Thermo Fisher Scientific, USA). After 48 and 72 h, the lentivirus in the culture medium was collected and infiltrated with 0.45 μm filters. The lentivirus was added to the culture medium with 8 μg/mL polybrene (Sigma) in VSMCs.

2.7. Transwell assay

As previous described, the 1×10^4/mL cells were suspended in serum-free medium after digestion with trypsin, and then seeded into the upper Boyden chamber (a filter with a 6.5-mm diameter and 8.0-μm pore size; Corning, Corning, NY, USA)[21]. The 0.8 mL serum free DMEM containing PDGF-BB (20 ng/mL) was applied for the lower chamber. After incubated at 37 °C under 5% CO_2 for 24 h, the cells invading through chamber membrane were washed with PBS for three times and immobilized in paraformaldehyde for 10 min. Then, the cells were stained with crystal violet for 30 min and counted under the microscope as the mean number of cells per 5 random fields for each assay.

2.8. Wound healing assay

Wound healing assay was utilized to evaluate the migration of cells. When grown to 90% confluence, the cells were scratched with three wound lines on the middle and both sides of the medium with 2.5 μL pipette tip, cultured in 5% CO_2 atmosphere at 37 °C. The wound width was observed and measured at 48 h. The wound width and area were analyzed using Digimizer.

2.9. EdU proliferation assay

The proliferation of cells was assessed by performing 5-ethynyl-20-deoxyuridine (EdU, KeyGEN BioTECH, Shanghai, China) incorporation assay according to the manufacturers' instructions. Total cellular nuclei were stained with DAPI. Immunofluorescence EdU positive cells were observed as green color under the Zeiss inverted fluorescent microscope (Zeiss LSM780, Carl Zeiss). And the EdU incorporation rate was presented as the ratio of EdU positive cells to total DAPI positive cells.

2.10. Immunofluorescence staining

VSMCs were fixed with 4% paraformaldehyde for 15 min, subsequently permeated with 0.5% Triton X-100 in PBS 10 min, followed by blocking in 5% goat serum in PBS at room temperature for 30 min, and incubated with the first antibody at 4 °C overnight. The arterial sections with retrieved antigens were blocked in 5% goat serum in PBS at room temperature for 30 min. Afterwards, the sections were incubated with the first antibody at 4 °C overnight. Appropriate fluorescence secondary antibody was applied to the cells/tissue at room temperature for 1.5 h. The 4′,6-diamidino-2-phenylindole (DAPI, C1005, Beyotime Biotechnology, Shanghai, China) was used to stain the nuclei. The images

were recorded through using a fluorescent microscope (Zeiss LSM780, Carl Zeiss).

2.11. Histology and immunohistochemistry assay

After fixation, the arterial segments were dehydrated, embedded in paraffin, and cut into 5-μm sections. The hematoxylin and eosin (H&E) and verhoeff's van gieson (EVG) staining were applied on artery sections for histopathologic features, including morphologic change and intimal hyperplasia.

Paraffin-embedded tissue sections were deparaffinized in xylene and rehydrate through a gradient of ethanol solutions followed by three times wash with PBS. Then, the antigens were retrieved by incubating sections with citrate buffer at 95 °C for 10 min. Next, the sections were blocked in 5% goat serum in PBS at room temperature for 30 min, followed by incubation with primary antibody at 4 °C overnight. After three times rinse with PBS, the sections were incubated with appropriate secondary antibody at room temperature for 1.5 h, followed by visualization with 3,3-diaminobenidine (DAB). The slides were counterstained with hematoxylin. The immunostained sections were recorded using a microscope.

2.12. Chromatin immunoprecipitation PCR (ChIP-PCR)

ChIP assays of VSMCs induced with PDGF-BB (20 ng/mL) for 2 and 6 h were performed as previous described protocol[21]. Briefly, the cells crosslinked with formaldehyde were collected for protein extraction, which was sheared to 300−1000 bp by sonication and immunoprecipitated with anti-SMYD3 or anti-H3K4me3. The same amount of non-specific IgG was performed as control. Immunoprecipitated protein−DNA complex was purified, followed by captured with protein-G beads. The multiple sets of primers spanning the transcription factor binding site on *Parp16* gene promoter were subjected to PCR analysis. Primer sequences were as follows: *Parp16*: 5′-CAGGACTGACTGCAGAGTGC-3′, and 5′-ACTCTGTAGCCCATGCTGAC-3′.

2.13. Co-immunoprecipitation (Co-IP)

For PARP16 immunoprecipitation, hVSMCs were transfected with lentivirus-mediated FLAG-PARP16 cDNA, followed by stimulation with 20 ng/mL PDGF-BB for 36 h. For ADP-ribose immunoprecipitation, hVSMCs were treated with 20 ng/mL PDGF-BB for 36 h. Then, cells were lysed in IP buffer (Beyotime, China) with protease inhibitors. The lysates were collected and centrifuged at 10,000×*g* for 10 min at 4 °C. The supernatants were incubated overnight at 4 °C with constant rotation with anti-FLAG antibody or anti-ADP-ribose binding agent, with corresponding IgG as control, after diluted to the same concentration by cold PBS. The samples were then incubated with Protein A/G Plus-Agarose (sc-2002, Santa Cruz, CA, USA) for 4 h at 4 °C with constant rotation. The immunoprecipitate complex were centrifuged, then washed five times and eluted with 1 × LDS buffer. Finally, the eluates were separated by SDS-PAGE and analyzed by Western blot.

2.14. Rat carotid artery balloon injury

All animal procedures conformed to the Guide for the Care and Use of Laboratory Animals were approved by Institutional Animal Care and Use Committee (IACUC), School of Pharmacy, Fudan University, Shanghai, China.

Carotid artery balloon injury was performed on male Sprague−Dawley rats (350−400 g). After anesthetized by an intraperitoneal injection of pentobarbital sodium diluted in 0.9% saline, the left carotid artery was exposed followed by a longitudinal incision made in the neck. A 2-F balloon catheter was inserted by an arteriotomy on the left external carotid artery. To induce arterial injury, the balloon was inflated at a pressure of 1.5 atm and passed in the common artery, repeating five times. After the balloon was carefully removed, the external carotid was ligated, and the blood flow was restored. The *Parp16* or *Smyd3* and control small interfering RNA (siRNA) dissolved in 30% Poloxamer solution was applied in the common artery. The sham control mice experienced the same procedures without injury. After 14 days, the left common carotid artery of animals was perfused with appropriate saline to remove the blood. The carotid artery was separated into two segments: one fixing in 4% paraformaldehyde was used for morphological analysis, and the other was used to measure the expression of related proteins.

2.15. Mice carotid artery ligation

Mice (22−25 g) were anesthetized and the carotid artery ligation was performed according to a protocol developed by Allagnat[21]. The left common carotid artery was dissected and ligated just below the carotid bifurcation with Prolene 8.0. The skin incision was subsequently closed and mice were cared to recover from anesthesia. EGCG at doses of 5 and 10 mg/kg/day was administered to mice by intraperitoneal injection once a day for 4 weeks. After mice were killed, the segments were collected and subsequent morphometric analyses were performed.

2.16. Statistical analysis

Experimental results are expressed as mean ± standard error of mean (SEM). Differences of means were analyzed by using one-way ANOVA with Tukey−Kramer *post hoc* test for multiple groups and unpaired Student's *t*-test for two groups. A P value < 0.05 is considered significant.

3. Results

3.1. PARP16 and ER stress are involved in SMCs proliferation and migration in vitro as well as in vivo neointimal hyperplasia

PDGF-BB is conventionally used to induce the SMCs proliferation and migration *in vitro*[22]. In the present study, PDGF-BB (20 ng/mL) was added in the rat vascular smooth muscle cells (rVSMCs) for 24 and 48 h. Interestingly, the expression of PARP16 was dramatically elevated in PDGF-BB-induced rVSMCs, as well as activation of three identified ER stress sensor PERK, IRE1α, and ATF6, and time-dependent activation of downstream signaling including BIP, spliced XBP-1, p-eIF2α, and ER structure marker calnexin (Fig. 1A and Supporting Information Fig. S1A). Consistent with this results, gene expression of multiple ER stress markers such as *Bip*, *Chop*, *Grp94*, *Ppi* was increased (Fig. 1B). Next, we further examined the expression of PARP16 in PDGF-BB-induced human aortic smooth muscle cells (hVSMC). The expression of PARP16 was time-dependently upregulated by PDGF-BB, accompanying the activation of three

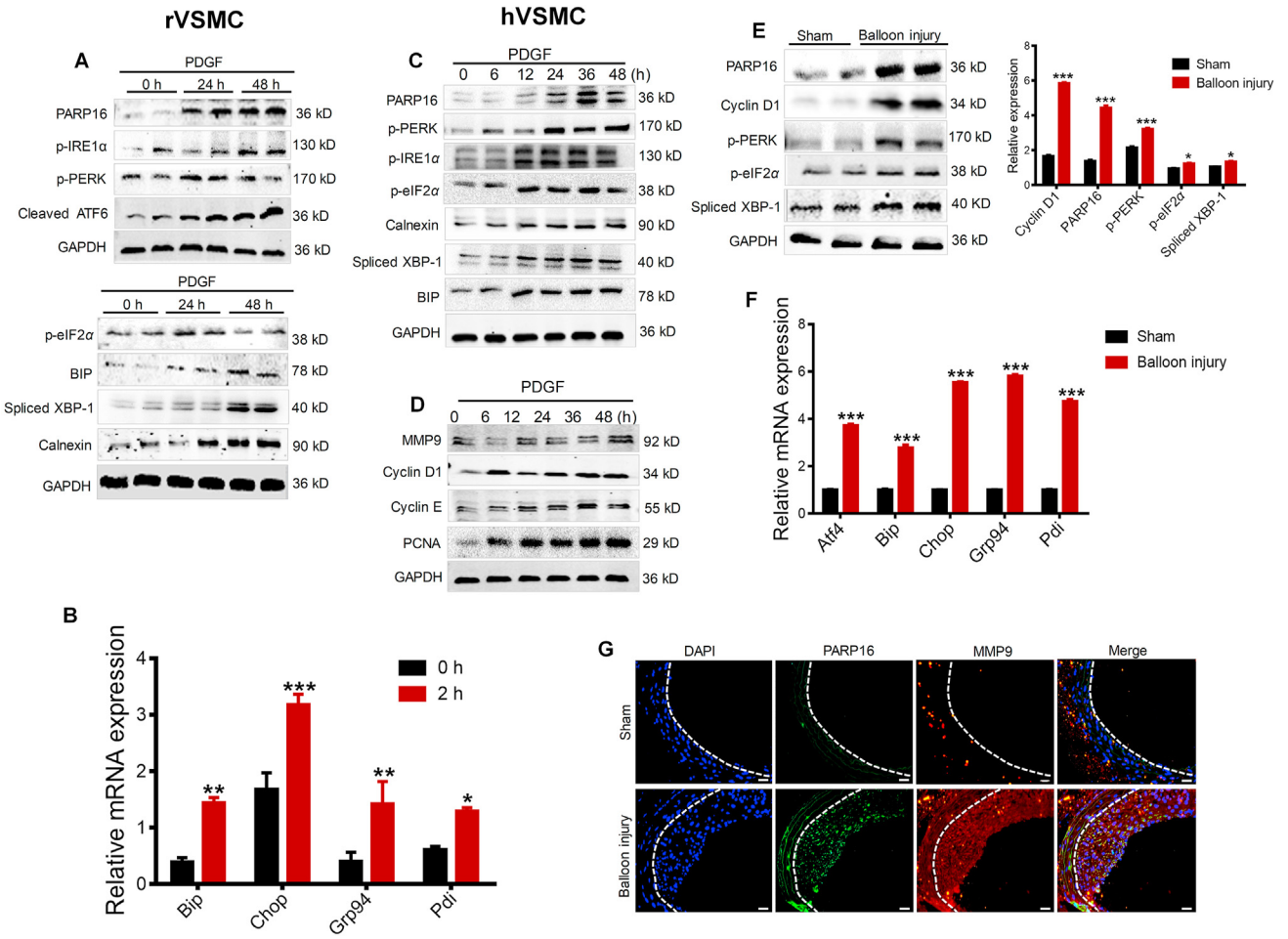

Figure 1 PARP16 and ER stress are involved in SMC proliferation and migration as well as neointima formation. (A) rVSMCs were treated with PDGF-BB (20 ng/mL) for 24 and 48 h, cell extracts were collected for determining the protein levels of PARP16 and activation of three signaling branches of UPR: PERK, IRE1α/XBP-1 and ATF6 by Western blot. (B) mRNA levels of UPR target genes in rVSMCs after PDGF-BB treatment for 2 h. All data are represented as mean ± SEM, $^{*}P < 0.05$, $^{**}P < 0.01$, $^{***}P < 0.001$ *vs.* 0 h, each acquired from three individual experiments. (C) The protein levels of PARP16 and activation of three signaling UPR branches PERK, IRE1α/XBP-1 and ATF6 were detected in hVSMCs after 20 ng/mL PDGF-BB stimulation for indicated time using Western blot; (D) Western blot analysis of MMP9, cyclin D1, cyclin E, PCNA protein levels in hVSMCs after 20 ng/mL PDGF-BB treatment. (E)−(G) PARP16 and ER stress were involved in intimal hyperplasia after rat carotid artery balloon injury. Western blot analysis of the PARP16, cyclin D1, p-PERK, p-IRE1α, spliced-XBP-1 protein levels in arteries from rat with sham operation or balloon injury for 14 days (E); mRNA levels of UPR target genes in arteries from rat with sham operation or balloon injury for 14 days (F); all data are represented as means ± SEM; $^{*}P < 0.05$, $^{***}P < 0.001$ *vs.* Sham group, $n = 7$ in each group. (G) Immunofluorescent staining with PARP16 (green) and MMP9 (red) in the rat carotid artery from the sham operation or 14-day post-balloon injury. All sections were counter-stained by DAPI to visualize nuclei (blue), scale bars: 100 μm.

ER stress sensor (Fig. 1C and S1B). Meanwhile, PDGF-BB-induced an increase in cell proliferation and migration markers such as MMP9, cyclin D1, cyclin E and PCNA (Fig. 1D and S1C). In addition, PARP16 was induced in arterial injury where neointimal VSMCs are known to be proliferative, and ER stress markers were also upregulated (Fig. 1E). Consistent with this, mRNA levels of multiple UPR target genes such as *Atf4*, *Bip*, *Chop*, *Grp94*, and *Pdi* were increased in balloon injured carotid artery (Fig. 1F). The immunofluorescence double staining also showed that the expressions of PARP16 and MMP9 were increased in balloon injured carotid artery (Fig. 1G). Above all, these results indicate that PARP16 and ER stress were involved in SMC proliferation and migration *in vitro* and *in vivo*.

3.2. *Deficiency of PARP16 reduces proliferation and migration and ER stress in PDGF-BB-induced rVSMC*

To determine whether PARP16 functions in SMC proliferation and migration, we knocked down *Parp16* using siRNA. Intriguingly, knocking down PARP16 expression could block PDGF-BB-induced the increase in protein levels of PCNA, MMP9, cyclin D1 and cyclin E (markers for cell proliferation and migration, Fig. 2A). Besides, silencing *Parp16* decreased activation of ER stress sensor p-PERK, p-IRE1α, and downstream signaling such as BIP, Spliced XBP-1, p-eIF2α, as well as ER structure marker calnexin in PDGF-BB-induced rVSMCs (Fig. 2B). As has been well documented that proliferation and

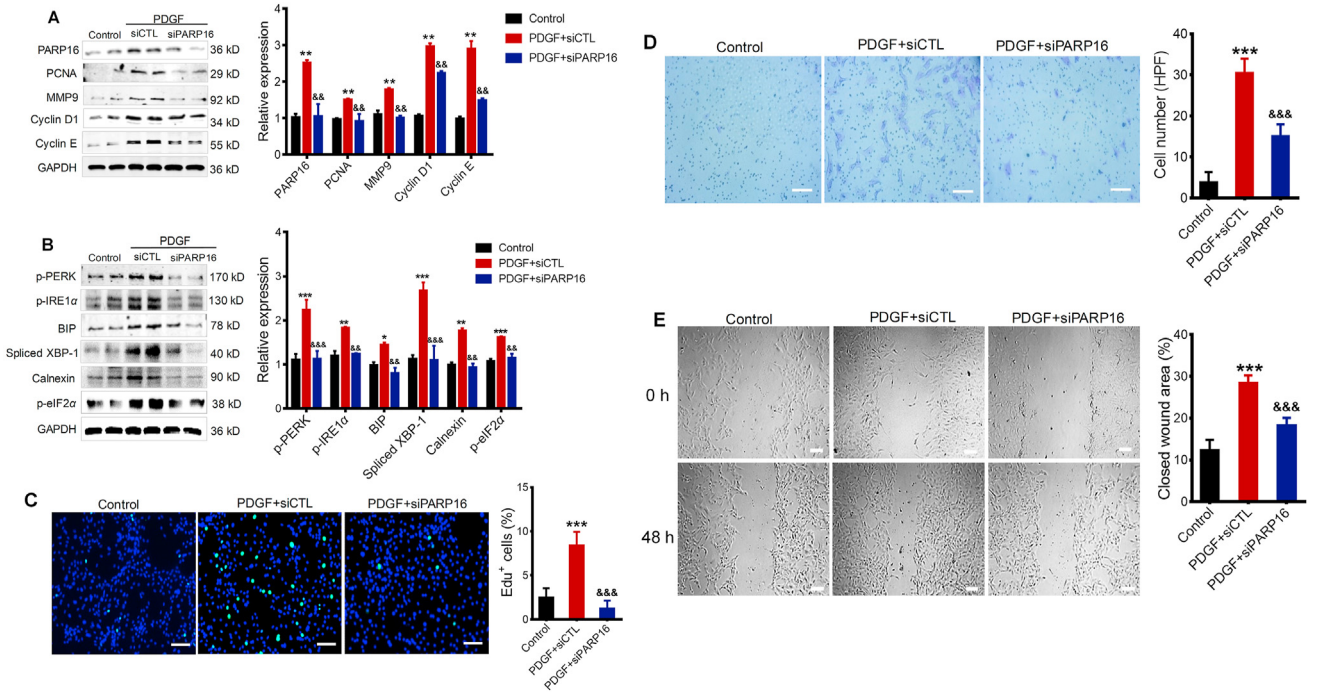

Figure 2 Deficiency of *Parp16* suppresses PDGF-BB-induced rVSMC proliferation and migration through ER stress. Following transfection with control siRNA (siCTL) or *Parp16* siRNA (siPARP16) for 72 h, rVSMCs were treated with 20 ng/mL PDGF for 24 h, cell extracts were collected for determining the protein levels of PARP16, PCNA, MMP9, cyclin D1, and cyclin E by Western blot (A); cell lysates were immunoblotted with p-PERK, p-eIF2α, BIP, p-IRE1α, spliced XBP-1 and calnexin antibodies (B). rVSMCs were transfected with *Parp16* siRNA (siPARP16) or control siRNA (siCTL) for 72 h, and then stimulated with 20 ng/mL PDGF-BB for 24 or 48 h, the EdU positive cells were showed green color and cell nuclei stained with DAPI showed blue color, scale bars: 200 μm (C); the migratory ability of rVSMCs was determined by Transwell assay, scale bars: 200 μm (D) and wound healing assay, scale bars: 400 μm (E). All data are represented as means ± SEM; $^{*}P < 0.05$, $^{**}P < 0.01$, $^{***}P < 0.001$ *vs.* control; $^{\&\&}P < 0.01$, $^{\&\&\&}P < 0.001$ *vs.* PDGF + siCTL, each acquired from three individual experiments.

migration of SMCs are major contributors to intimal hyperplasia[23], we examined the impact of PARP16 on rVSMC proliferative and migratory capacities. EdU positive cells were significantly increased in the presence of PDGF-BB but were lower in rVSMC transfected with *Parp16* siRNA, indicating that the knocking down of PARP16 had a suppressive effect on rVSMCs proliferation (Fig. 2C). Next, we tested whether PARP16 is important for cell migration. As expected, the Transwell and wound healing assay indicate that silencing of *Parp16* greatly prevented rVSMC migration induced by PDGF-BB (Fig. 2D and E). Taken together, the results demonstrate that the knocking down the expression of PARP16 could decrease the SMC proliferative and migratory capacities.

3.3. *Inhibition of PARP16 reduces proliferation and migration and ER stress in PDGF-BB-induced rVSMC*

Epigallocatechin-3-gallate (EGCG) is the most bioactive catechin in green tea[24,25]. Recently, EGCG was described as potential inhibitor of PARP16[26], we further determined the effect of EGCG on the rVSMCs proliferation and ER stress. Surprisingly, we found that rVSMCs treated with EGCG (30 μmol/L) showed remarkably reduced expression of PCNA, cyclin E, cyclin D1, and MMP9 in response to PDGF-BB (Fig. 3A), and EGCG also decreased the expression of p-PERK, p-IRE1α, Spliced XBP-1, BIP, and p-eIF2α (Fig. 3B), suggesting that inhibition of PARP16 mitigated ER stress, as well as proliferation and migration of rVSMCs. Likewise, EGCG decreased cell proliferation (Fig. 3C) and migration (Fig. 3D and E) in PDGF-stimulated rVSMCs. Taken together, these results support that the inhibition of PARP16 could decrease the SMC proliferative and migratory capacities through mediating ER stress.

3.4. *Deficiency or inhibition of PARP16 reduces proliferation and migration-related proteins and ER stress in PDGF-BB-induced hVSMC*

We further determined the effect of PARP16 in PDGF-BB-induced hVSMC. As expected, knocking down *Parp16* expression could block PDGF-BB-induced increase in protein levels of PCNA, cyclin D1 and cyclin E (Supporting Information Fig. S2A). Besides, the deficiency of PARP16 decreased the expression of ER stress markers such as p-PERK, p-IRE1α, p-eIF2α, and spliced XBP-1 in PDGF-BB-induced hVSMCs (Fig. S2B). Similarly, ECGC also decreased expression of cyclin E, PCNA, and cyclin D1 in response to PDGF-BB (Fig. S2C), as well as expression of p-PERK, p-IRE1α, p-eIF2α, and spliced XBP-1 (Fig. S2D), suggesting that blockade of PARP16 mitigated ER stress, proliferation and migration of hVSMCs. These results are in consistent with those in rVSMC, further identified an effect of PARP16 on SMC proliferation and migration through ER stress.

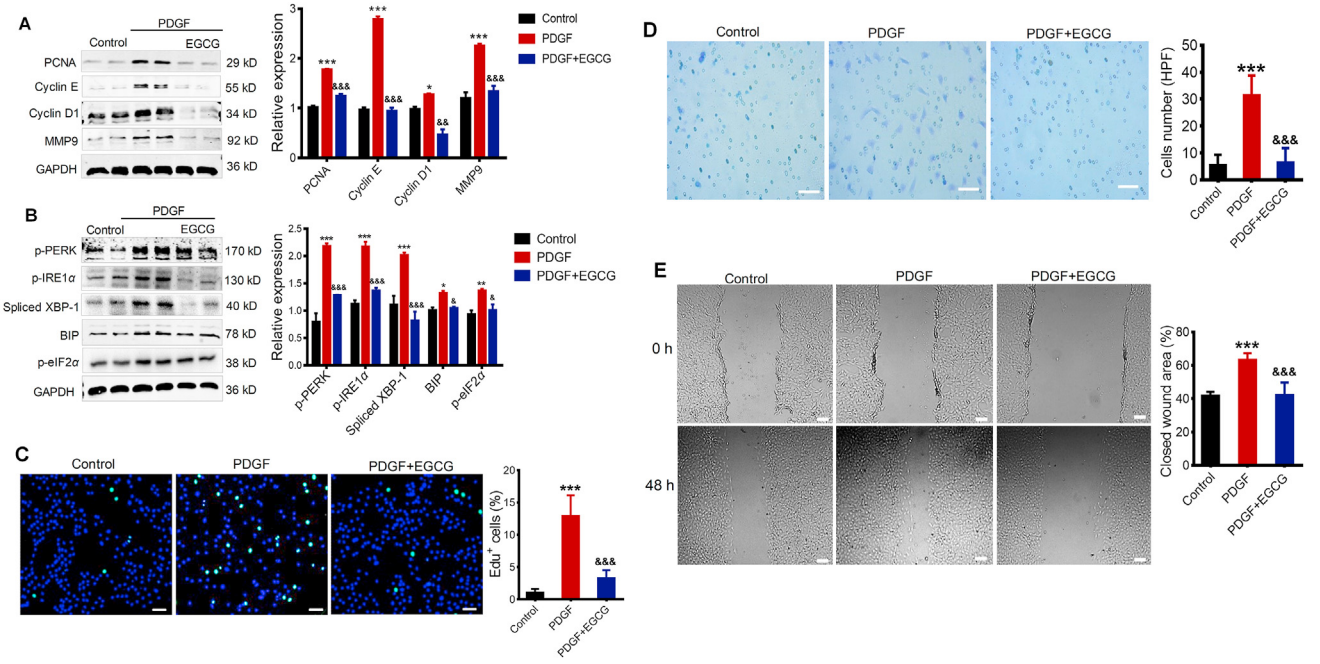

Figure 3 Inhibition of PARP16 alleviates PDGF-BB-induced rVSMC proliferation and migration through ER stress. Pretreated with EGCG (30 μmol/L) for 4 h, rVSMCs were treated with 20 ng/mL PDGF-BB for 24 h, cell extracts were collected for determining the protein levels of PCNA, cyclin E, cyclin D1 and MMP9 by Western blot (A); the protein levels of two branches PERK, IRE1α/XBP-1 of UPR signaling were determined by Western blot (B); the EdU positive cells showed green color and cell nuclei stained with DAPI showed blue color, scale bars: 200 μm (C); the migratory ability of rVSMCs was determined by Transwell assay, scale bars: 200 μm (D) and wound healing assay, scale bars: 400 μm. (E). All data are represented as means ± SEM; $^{*}P < 0.05$, $^{**}P < 0.01$, $^{***}P < 0.001$ *vs.* control; $^{\&}P < 0.05$, $^{\&\&}P < 0.01$, $^{\&\&\&}P < 0.001$ *vs.* PDGF, each acquired from three individual experiments.

3.5. Overexpression of PARP16 induces SMC proliferation and migration accompanying ER stress

We have verified that inhibiting or silencing PARP16 could alleviate VSMC proliferation and migration induced by PDGF-BB. Hence, to confirm that whether elevated PARP16 can lead to VSMCs proliferation and migration, we overexpressed PARP16 in rVSMCs by applying a lentivirus-based transduction method, Western blot analysis confirmed the overexpression of PARP16 in rVSMCs (Fig. 4A). We found that overexpressed PARP16 resulted in ER stress markers, as well as notable augmented expression of proliferation and migration markers (Fig. 4A and B). rVSMCs overexpressed PARP16 were then subjected to functional assays including cell proliferation and migration. It was important to note that rVSMC migration and proliferation were significantly enhanced by PARP16 overexpression as demonstrated by wound-healing (Fig. 4C), Transwell migration assays (Fig. 4D) and EdU incorporation analysis (Fig. 4E). Collectively, overexpression of PARP16 induced SMCs proliferation and migration accompanying ER stress.

3.6. PARP16 activates PERK and IRE1α by selectively ADP-ribosylating PERK and IRE1α during the PDGF-stimulating hVSMC

Next, to identify how the ER stress is activated by PARP16, we generated a FLAG-tagged PARP16 (FLAG-PARP16) plasmid and transiently expressed it in hVSMCs. Immunofluorescence images confirmed PARP16 co-localized with the ER structure marker calnexin (Fig. 4F). Because PARP16 is an effective regulator of ER stress sensor PERK and IRE1α, to clarify the interaction between the PARP16 and ER stress sensor, cell lysates were immunoprecipitated with antibody against FLAG-PARP16. Co-IP results showed that PARP16 could interact with PERK and IRE1α in PDGF-induced hVSMC (Fig. 4G). It is generally known that ADP-ribosylation by PARP16 directly activates PERK and IRE1α. To determine whether the ADP-ribosylation of PERK and IRE1α was upregulated under PDGF, we used Co-IP to examine the level of ADP-ribosylation of PERK and IRE1α. Our result exhibits PDGF resulted in an increased ADP-ribosylation of PERK and IRE1α, suggesting that ADP-ribosylation by PARP16 was sufficient to activate PERK and IRE1α (Fig. 4H). Together, ER-associated tail-anchored protein PARP16 induced SMC proliferation and migration at least in part by selectively ADP-ribosylating PERK and IRE1α during the UPR, and that such modification is required for activation of PERK and IRE1α.

3.7. ER stress contributes to PDGF-mediated proliferation and migration of SMCs

It has also been reported that tauroursodeoxycholic acid (TUDCA) can decrease ER stress[27,28]. Next, the effect of TUDCA on SMCs was investigated. Indeed, in our study, treatment with TUDCA could ameliorate the expression of PCNA, cyclin D1, cyclin E in response to PDGF-BB in a dose-dependent manner in rVSMCs and hVSMCs (Supporting Information Fig. S3A). On the other hand, TUDCA variously abrogated the increase in the above ER stress markers in PDGF-induced SMCs (Fig. S3B). Therefore, the findings suggest that TUDCA inhibited both the proliferation and migration of SMCs by decreasing ER stress. Brefeldin A (BFA), a

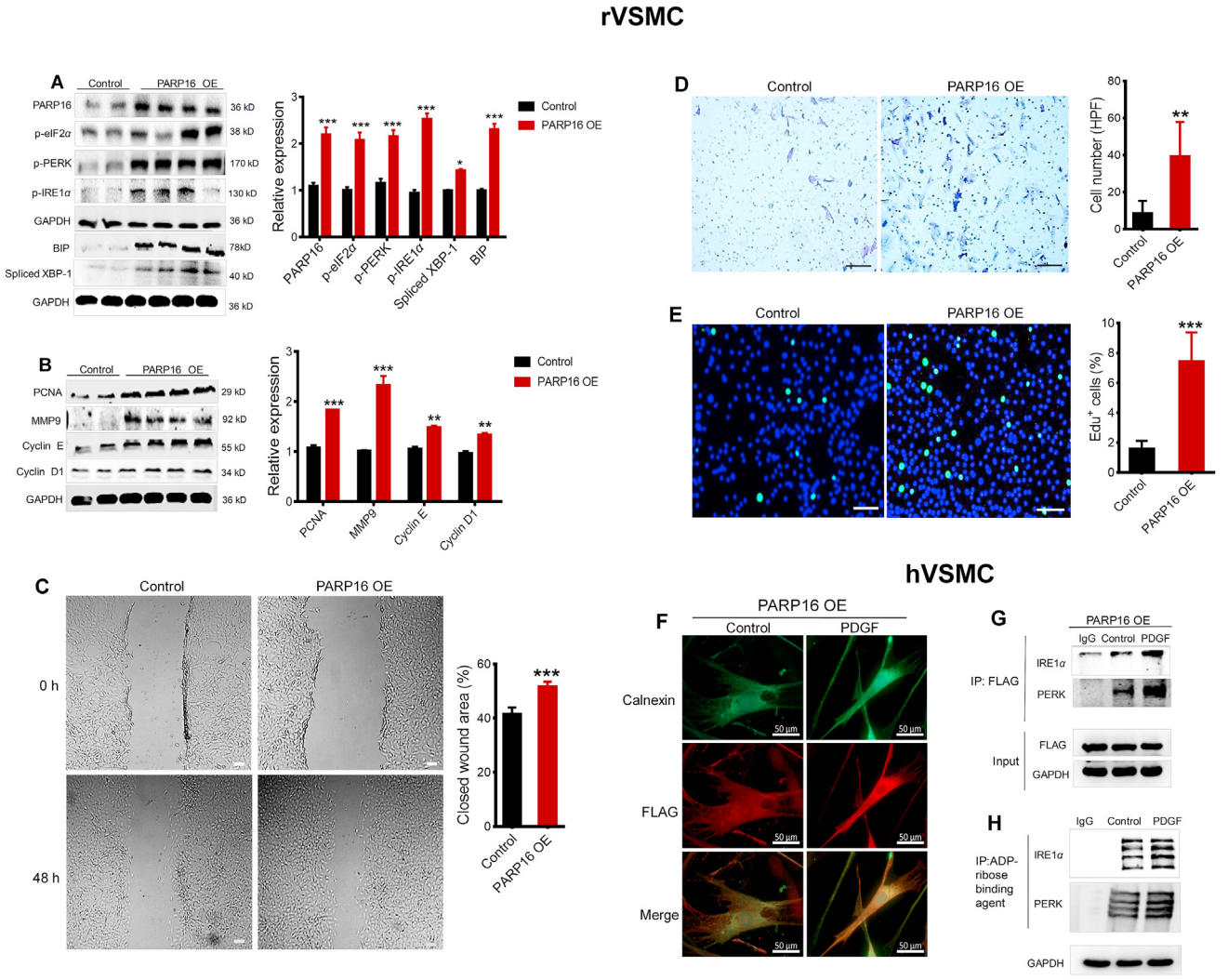

Figure 4 Overexpression of PARP16 results in VSMC proliferation and migration accompany with ER stress. rVSMCs were transfected with lentivirus-mediated *Parp16* cDNA (PARP16 OE) or vector (Control) for 72 h, cell lysates were immunoblotted with antibodies against PARP16, p-PERK, p-eIF2α, p-IRE1α, spliced XBP-1, and BIP (A); PCNA, MMP9, cyclin E and cyclin D1 (B); rVSMCs migration ability was tested by wound healing assay, scale bars: 400 μm. (C) and Transwell assay, scale bars: 200 μm (D); rVSMCs proliferation ability was detected by EdU assay, scale bars: 200 μm (E); All data are represented as means ± SEM; $*P < 0.05$, $**P < 0.01$, $***P < 0.001$ *vs.* control, each acquired from three individual experiments. (F)−(H) PARP16 selectively ADP-ribosylated PERK and IRE1α during the UPR. hVSMCs with overexpression FLAG-PARP16 were treated PDGF-BB for 36 h, the PARP16 localization was demonstrated by co-immunostaining with calnexin, scale bars: 50 μm. (F); Coimmunoprecipitation using antibody against FLAG in lysates of hVSMCs induced by PDGF (G); Coimmunoprecipitation using anti-ADP-ribose binding reagents in lysates of PDGF-BB-induced hVSMCs (H).

known ER stress activator in UPR pathway, exhibited an increase in protein expression of ER stress markers served as a positive control in the assay (Supporting Information Fig. S4A). Meanwhile, proliferation and migration-related markers such as PCNA, cyclin D1, cyclin E and MMP9 were increased in different degrees (Fig. S4B). Together, we verified the role of ER stress in SMCs proliferation and migration induced by PDGF.

3.8. Blocking PARP16 effectively mitigates intimal hyperplasia and ER stress in balloon-injured rat carotid arteries

In vitro gain- and loss-of-function assays suggested a unique role of PARP16 in VSMC migration and proliferation. Therefore, we next examined the functional role of PARP16 in neointima formation *in vivo* under pathological conditions. To explore the *in vivo* efficacy of silencing *Parp16*, rat carotid arteries were harvested on Day 14 after balloon injury, sectioned and immunostained with hematoxylin and eosin (H&E, Fig. 5A). The decreased intima-to media (I/M) thickness ratio of carotid arteries from *Parp16* siRNA treated rat was observed, compared with control siRNA (Fig. 5B). We confirmed that PARP16 expression was significantly depleted in aorta incubate with *Parp16* siRNA, accompanying a markedly reduced expression of ER stress marker proteins (Fig. 5C). Besides, knocking down of *Parp16* significantly inhibited the injury-induced increase in cyclin D1, PCNA, cyclin E, MMP9, and VCAM-1 expression in the neointima of carotid arteries (Fig. 5D), which stated that knocking down *Parp16* may inhibit intimal hyperplasia through ER stress. Moreover, the expression of cyclin D1 in *Parp16* siRNA-treated group was also alleviated in the injured-induced vascular intima

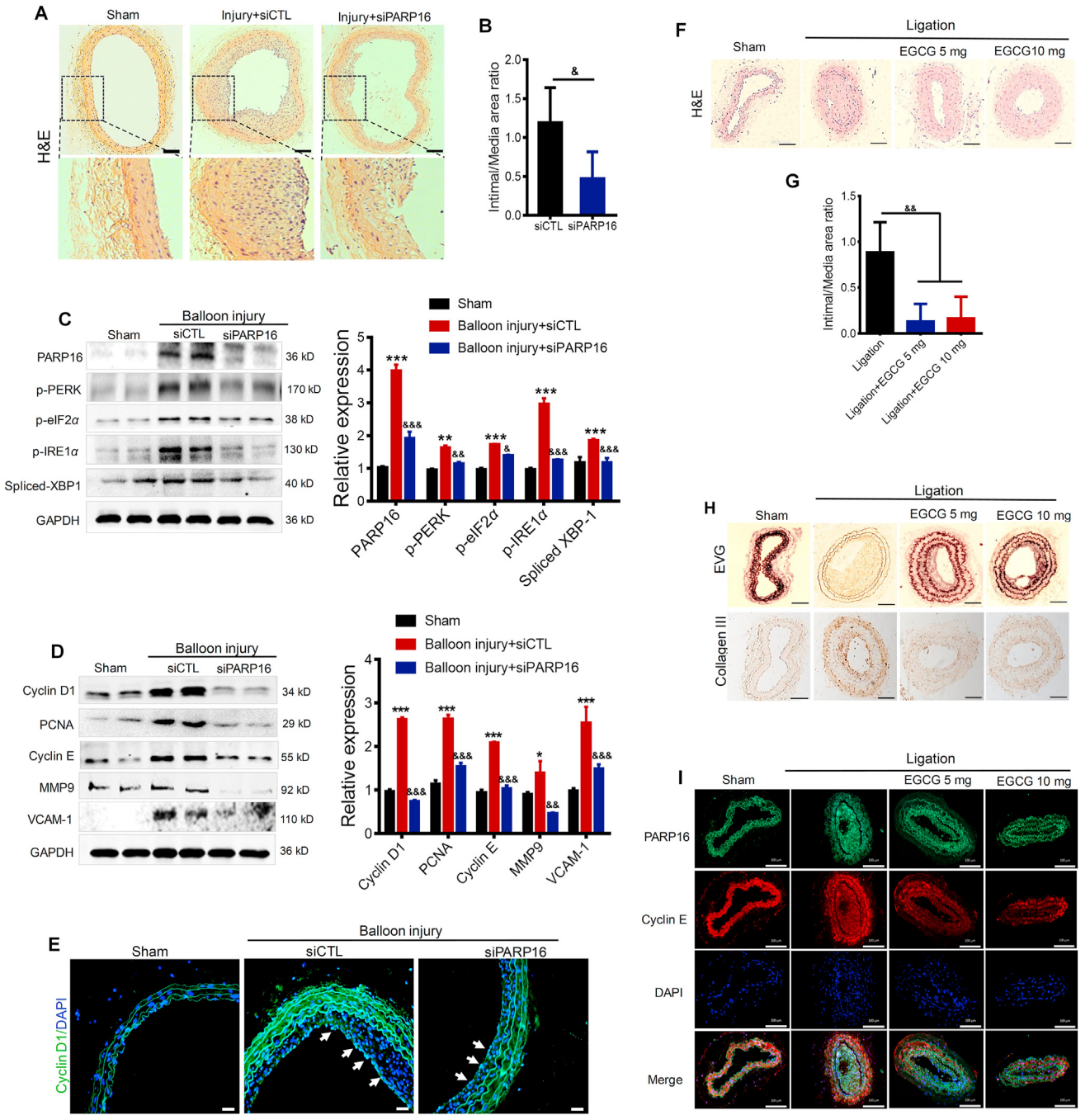

Figure 5 Blocking of PARP16 mitigates intimal hyperplasia after balloon injury. (A)−(E) Knocking down of *Parp16* mitigated intimal hyperplasia after rat carotid artery balloon injury. Representative H&E-stained sections in carotid arteries from rat that underwent sham, balloon injury, and *Parp16* siRNA (siPARP16) treatment for 14 days after balloon injury, scale bars: 200 μm. (A); treatment with siPARP16 led to a reduction of neointima/media ratio (I/M), $^{\&}P < 0.05$, $n = 10$/group (B); Western blot analysis of the PARP16, p-PERK, p-eIF2α, p-IRE1α, and spliced XBP-1 protein levels in arteries from rat that underwent sham, balloon injury, and siPARP16 treatment for 14 days after balloon injury (C); Western blot analysis of the cyclin D1, PCNA, MMP9, cyclin E and VCAM-1 protein levels in arteries from rat carotid arteries (D); immunofluorescent staining with anti-cyclin D1 in rat carotid arteries, the arrowheads indicate the positive cells staining in intimal hyperplasia, scale bars: 100 μm (E); above all Western blot data are represented as mean ± SEM, $^{*}P < 0.05$, $^{**}P < 0.01$, $^{***}P < 0.001$ *vs.* sham; $^{\&\&}P < 0.01$, $^{\&\&\&}P < 0.001$ *vs.* balloon injury + siCTL, $n = 8$/group. (F)−(J) The inhibiting PARP16 abrogated intimal hyperplasia in carotid artery ligation mice. Carotid artery ligation mice were administered 5 and 10 mg/kg/day EGCG by oral gavage 28 days until the end of the experiment. Representative hematoxylin and eosin (H&E) staining of partial left carotid arteries from mouse with sham, ligation and EGCG treatment, scale bars: 100 μm (F); EGCG treatment decreased neointima/media ratio (I/M), $^{\&\&}P < 0.01$, $n = 10$/group (G); representative EVG staining and immunohistochemical staining of collagen III of partial left carotid arteries from mouse with sham, ligation or EGCG treatment, scale bars: 100 μm (H); immunofluorescent staining with PARP16 (green) and cyclin E (red) of partial left carotid arteries from different-treated mice, scale bars: 100 μm (I).

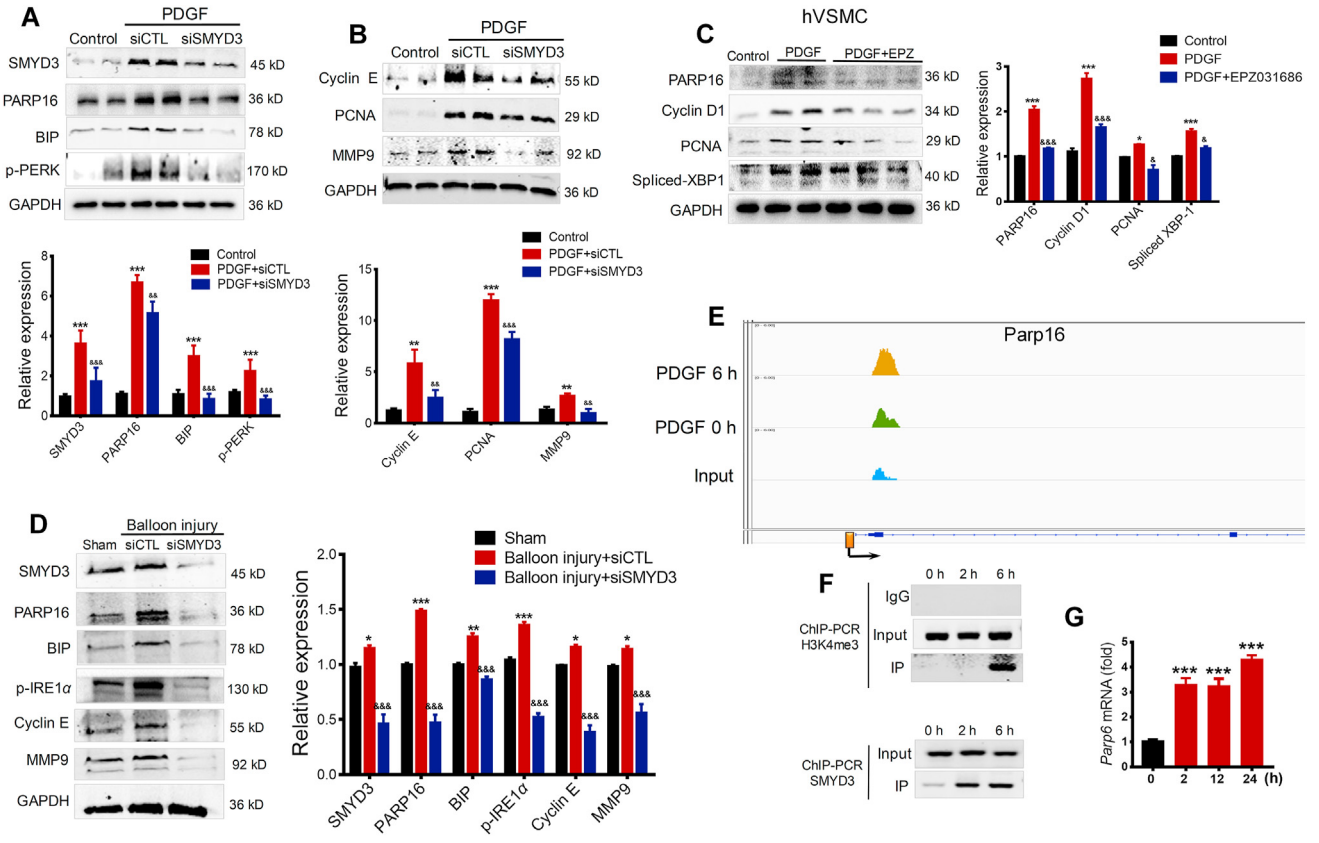

Figure 6 Methyltransferase SMYD3 binding to promoters of *Parp16* can lead to an increased H3K4me3 level and promotes SMCs proliferation and migration. (A) and (B) Knocking down of *Smyd3* decreased PARP16 expression and ER stress. Following transfection with control siRNA (siCTL) or *Smyd3* siRNA (siSMYD3), rVSMCs were treated with 20 ng/mL PDGF for 24 h, Western blot analysis for SMYD3, PARP16, BIP, p-PERK protein levels (A); Western blot analysis for cyclin E, PCNA, and MMP9 protein expressions in rVSMCs (B); (C) the inhibition of SMYD3 decreased PARP16 expression. Pretreated with EPZ031686 (40 μmol/L) for 4 h, hVSMCs were treated with 20 ng/mL PDGF-BB for 36 h, cell extracts were collected for determining the protein levels of PARP16, PCNA, cyclin D1 and spliced XBP-1 by Western blot; all data are represented as mean ± SEM, $^{*}P < 0.05$, $^{**}P < 0.01$, $^{***}P < 0.001$ *vs.* control; $^{\&}P < 0.05$, $^{\&\&}P < 0.01$, $^{\&\&\&}P < 0.001$ *vs.* PDGF or PDGF + siCTL, each acquired from three individual experiments. (D) Western blot analysis of the SMYD3, PARP16, p-IRE1α, BIP, cyclin E, and MMP9 protein levels in carotid arteries from rat that underwent sham, balloon injury, and siSMYD3 treatment for 14 days after balloon injury, data are represented as mean ± SEM; $^{*}P < 0.05$, $^{**}P < 0.01$, $^{***}P < 0.001$ *vs.* sham; $^{\&\&\&}P < 0.001$ *vs.* balloon injury + siCTL, $n = 6$/group. (E)−(G) SMYD3 binding to promoters of *Parp16* could lead to an increased H3K4me3 level and gene expression in PDGF-BB-induced rVSMCs. (E) Integrative Genomics Viewer (IGV) showed a signal of ChIP-seq (H3K4me3) at PARP16 coding gene's locus in control and PDGF-induced rVSMCs (6 h). The *Y*-axis was normalized to the same scale. The black arrow means primer pairs used for ChIP-PCR in panel F. (F) ChIP-PCR using either H3K4me3 or SMYD3 antibody showed H3K4me3 and SMYD3 enrichment at the promoter of *Parp16* in PDGF-induced VSMCs for 2 and 6 h. (G) RT-qPCR to quantify mRNA level of *Parp16* upon induction of PDGF in rVSMCs. All data shown are representative of data from at least three different replicates; $^{***}P < 0.01$ *vs.* control.

showed by immunofluorescence staining (Fig. 5E). These results suggest that knocking down of *Parp16* exhibited an inhibitory effect on cell proliferation through ER stress, and may provide an effective strategy for prevention of restenosis after angioplasty.

3.9. Inhibiting PARP16 attenuates intimal hyperplasia in carotid artery ligation mice

As described above, our *in vitro* data supported the role of PARP16 in promoting VSMC proliferation. Therefore, we aimed to determine whether inhibition of PARP16 using EGCG could influence the neointimal thickening in mice carotid artery ligation model[29]. After 28 days of administration with 5 and 10 mg/kg/day dosages of EGCG, the left common carotid artery was harvested and stained with H&E (Fig. 5F). The neointima formed in response to carotid artery ligation was significantly reduced in 5 and 10 mg/kg EGCG-treated mice compared with the ligation counterparts (Fig. 5G). Similarly, Verhoeff's van Gieson (EVG) staining and immunohistochemistry double-checked the protective effect of EGCG on the injury-induced elastic fibers and fibrosis (Fig. 5H). Immunofluorescence staining of PARP16 and cyclin E further revealed that the PARP16 inhibition attenuated VSMC proliferation after ligation injury (Fig. 5I). Together, these findings indicate that PARP16 participated in intimal hyperplasia as a positive role, providing an effective agent to ameliorate intimal hyperplasia.

3.10. Identifying Parp16 as potential target gene of methyltransferase SMYD3

From the above results, we concluded that PARP16 promotes intimal hyperplasia through mediating ER stress, next we explored how the PARP16 was upregulated in response to PDGF. SMYD3 is a histone methyltransferase and acts as an "amplifier" or "potentiator" of genes transcription[30]. Surprisingly, we found SMYD3 expression was increased after PDGF treatment (Fig. 6A), illustrating that SMYD3 was also involved in the PDGF-induced rVSMCs proliferation and migration. Then, we transfected rVSMCs with *Smyd3* siRNA and found that knockdown of *Smyd3* decreased expression of PARP16 and ER stress markers (Fig. 6A), which suggesting SMYD3 may be the direct upstream regulator of PARP16. Consistently, knocking down of *Smyd3* also decreased proliferation markers, such as PCNA, MMP9 and cyclin E (Fig. 6B). Meanwhile, SMYD3 specific inhibitor EPZ031686 attenuated PARP16 expression with reduced PCNA, cyclin D1, and spliced XBP-1 expression in PDGF-induced hVSMC (Fig. 6C). In addition, we next examined the functional role of SMYD3 in neointima formation *in vivo* under pathological conditions. We confirmed that PARP16 expression was significantly depleted in aorta incubate with *Smyd3* siRNA, accompanying a reduced expression of ER stress marker proteins, MMP9 and cyclin E in the neointima of carotid arteries (Fig. 6D), which stated that knockdown of *Smyd3* may inhibit ER stress through suppressing PARP16 expression. Furthermore, we profiled levels of H3K4me3 by ChIP-seq in PDGF-induced rVSMCs for 6 h, an apparent increase of H3K4me3 signal was shown near the annotated TSS of *Parp16* gene (Fig. 6E), consistent with SMYD3's methyltransferase activity on H3K4. The DNA binding domain of SMYD3 specifically recognizes 5′-CCCTCC-3′ or 5′-CCCCTC-3′[17]. Interestingly, the promoter region (2 kilobase upstream of the transcription start site, or TSS) of *Parp16* contains 6 potential SMYD3 binding sites. In PDGF-treated rVSMCs, the increase of SMYD3 and H3K4me3 levels near the promoter of *Parp16* was validated by ChIP-PCR (Fig. 6F). Accordingly, the mRNA level of *Parp16* was markedly increased after PDGF treatment (Fig. 6G). These data indicate that SMYD3 transcriptionally promotes *Parp16* by epigenetic modification.

4. Discussion

In this study, we found that PDGF can upregulate PARP16 expression in VSMCs, accompanying activation of UPR, including PERK and IRE1α pathways. Importantly, we demonstrated for the first time that the inhibition or knockdown of PARP16 reduced PDGF-induced SMC proliferation and migration and intimal hyperplasia. These results indicate that blocking of PARP16 regulates the UPR balance to alleviate the process of neointima formation. Moreover, our study further provides the first evidence that SMYD3, an epigenetic writer, possibly played a significant role in promoting VSMC proliferation and migration at least partially by directly binding and transcriptionally activating PARP16.

Initially, ER stress activates a signaling pathway that leads to halting of protein translation and molecular chaperones to restore normal functions of the cells[31]. UPR is a compensatory reaction to ER stress, which is one of the endogenous sources of cellular stress characterized by an accumulation of misfolded or unfolded proteins in the ER[32]. Specifically, UPR has mainly three signaling pathways by sensor proteins: PERK, IRE1α and ATF6 pathways, by which additional sources of ER stress were alleviated and chaperons were induced for an increase in protein folding capacity and degradation in misfolded or unfolded proteins. Activation of the UPR has been suggested to be involved in vascular remodeling[12,33]. Most importantly, accumulating evidence indicates that activation of all branches of the UPR is associated with neointima formation after vascular injury and with PDGF-BB-induced proliferation, migration and inflammation in VSMCs[34], suggesting inhibition of ER stress as a promising therapeutic strategy in neointima formation after vascular injury[12,35]. Our present data also demonstrate that ER stress was induced in the neointima formation after vascular injury and PDGF-BB-induced VSMCs, mainly including PERK, IRE1α and ATF6 pathways. In contrast, using ER stress inhibitor TUDCA to the regulation of ER stress reduced VSMC proliferation and migration, which further verified that ER stress is a promising therapeutic target for vascular proliferative diseases.

PARP16 has been reported to have a role in both the nucleocytoplasmic shuttling through its mono-ADP-ribosylation and in the UPR through its ability to ADP-ribosylate Kapβ1, which has been implicated in regulating the ER quality control for promoting ER-associated degradation[15,36]. Accumulating evidence has clarified the close association between PARP16 and UPR. For another instance, PARP16 has been reported as an effective activator of ER stress sensor PERK and IRE1α through increasing their kinase activities and endonuclease activity of IRE1α. In this study, we have demonstrated ER-associated tail-anchored protein PARP16 induces SMC proliferation and migration by selectively ADP-ribosylating PERK and IRE1α during the UPR, and that such modification is required for activation of PERK and IRE1α. On contrary, inhibition or knocking down of PARP16 led to dramatic impairment of VSMCs proliferation and migration, as well as alleviation in intimal hyperplasia induced by injury or ligation, at least partly through mediating ER stress. Moreover, knocking down of PARP16 also attenuated the expression of the inflammatory mediator and collagen III after injury. Collectively, this suggests that disruption of PARP16 suppressed the neointima formation by impairing the proliferation of neointimal cells and reducing the production of the extracellular matrix. These results indicate that agents targeting PARP16, such as EGCG or gene intervention silencing *Parp16*, provide new ideas for clinic prevention of intimal hyperplasia. At the same time, it is important to note that EGCG is unstable due to rapid oxidation[37] and is highly nonspecific and targets a wide array of biological systems, the observed effects of EGCG could be nonspecific and indirect. Using EGCG as PARP16 inhibitor has unavoidable limitations, so specific PARP16 inhibitor need be further developed.

SMYD3, an epigenetic writer, has been reported to play significant roles in tumor proliferation, invasion and migration[38,39]. In present study, we found the expression of SMYD3 was upregulated in PDGF-BB-induced VSMC proliferation and migration. On the contrary, knockdown of *Smyd3* blocked proliferation and migration of VSMCs, as well as decreased PARP16 expression. Further, the knocking down of *Smyd3* significantly depleted PARP16 expression in aorta, accompanied with the reduced expression of ER stress and proliferation and migration markers in the neointima of carotid arteries, which stated that knocking down *Smyd3* may inhibit ER stress through suppressing PARP16 expression. In addition, previous studies have indicated that SMYD3 could catalyze histone modification, mainly bi/trimethylation of H3K4, to activate the transcription of multiple

target genes[17]. In support of this idea, we provided a supposing that upregulation of PARP16 is attributed to promoter H3K4 methylation status regulated by SMYD3. Interestingly, an apparent increase of H3K4me3 signal was shown near the annotated TSS of *Parp16* gene in PDGF-induced VSMCs compared to control cells by ChIP-seq, consistent with SMYD3's methyltransferase activity on H3K4. We searched for the promoter region (2 kilobases upstream of TSS) of *Parp16* containing 6 potential SMYD3 binding sites, thus, we further validated the increase of H3K4me3 levels near the promoter of *Parp16*. After that, we explored whether SMYD3 was a direct upstream regulator of *Parp16*. Our ChIP analysis confirmed the direct binding of SMYD3 to *Parp16*'s promoter regions, and transcriptionally activated PARP16 to promote VSMC proliferation and migration, providing a previous unestablished association between SMYD3 and PARP16. Those data indicated that SMYD3 transcriptionally promotes PARP16 expression by epigenetic modification. Our results agree with those of previous work, SMYD3 positively influences gene expression by mediating H3K4me3 recruitment at the proximal promoter of target genes[40,41]. Whereas in our study, we have not clarified whether other methyltransferases could regulate expression of PARP16 separately or jointly with SMYD3, which need further investigation in our future work.

5. Conclusions

In this study, we firstly found PARP16, a tail-anchored ER transmembrane protein, played a novel and key role in intimal hyperplasia likely through regulating the UPR of ER. In contractile VSMCs, SMYD3 and PARP16 are expressed at a low level. In contrast, in response to the stimuli that promote VSMC dedifferentiation and proliferation such as PDGF-BB, SMYD3 expression is induced, thereby initiating H3K4me3 enrichment on the promoter of PARP16 and consequently activating its transcription, resulting in ER and migration and proliferation of VSMC. To the best of our knowledge, we discovered SMYD3−PARP16 signal axis as a novel and important factor in regulating intimal hyperplasia for the first time. The intervention of either SMYD3 or PARP16 ameliorated VSMC proliferation and migration, shedding new light on prevention strategy for neointimal hyperplasia.

Acknowledgments

This work was supported by grants from the National Natural Science Foundation of China (Nos. 81673428 and 81872861). We thank Genergy Biotech (Shanghai) Co., Ltd. (China) for the deep sequencing service.

Author contributions

Fen Long performed the majority of experiments, analyzed the data, and drafted the paper. Di Yang, Jinghua Wang, and Qing Wang performed partial experiments and acquired the data. Ting Ni and Gang Wei analyzed the ChIP-seq data. Xinhua Liu and Yizhun Zhu designed the study, supervised the experiments, revised the manuscript and gave the final approval of the manuscript. All authors read and approved the manuscript as submitted.

Conflicts of interest

The authors declare no conflicts of interest.

Appendix A. Supporting information

Supporting data to this article can be found online at https://doi.org/10.1016/j.apsb.2020.12.010.

References

1. Marcucci G, Accrocca F, Giordano A, Antonelli R, Gabrielli R, Siani A. Results of surgical repair of carotid in-stent restenosis. *J Cardiovasc Surg* 2012;**53**:707−14.
2. Jang IK, Bouma BE, Kang DH, Park SJ, Park SW, Seung KB, et al. Visualization of coronary atherosclerotic plaques in patients using optical coherence tomography: comparison with intravascular ultrasound. *J Am Coll Cardiol* 2002;**39**:604−9.
3. Kipshidze N, Dangas G, Tsapenko M, Moses J, Leon MB, Kutryk M, et al. Role of the endothelium in modulating neointimal formation-vasculoprotective approaches to attenuate restenosis after percutaneous coronary interventions. *J Am Coll Cardiol* 2004;**44**:733−9.
4. Hansson GK. Inflammation and atherosclerosis: the end of a controversy. *Circulation* 2017;**136**:1875−7.
5. Owens GK, Kumar MS, Wamhoff BR. Molecular regulation of vascular smooth muscle cell differentiation in development and disease. *Physiol Rev* 2004;**84**:767−801.
6. De Labriolle A, Bonello L, Lemesle G, Steinberg DH, Roy P, Xue ZY, et al. Clinical presentation and outcome of patients hospitalized for symptomatic in-stent restenosis treated by percutaneous coronary intervention: comparison between drug-eluting stents and bare-metal stents. *Arch Cardiovasc Dis* 2009;**102**:209−17.
7. Walter P, Ron D. The unfolded protein response: from stress pathway to homeostatic regulation. *Science* 2011;**334**:1081−6.
8. Pakos-Zebrucka K, Koryga I, Mnich K, Ljujic M, Samali A, Gorman AM. The integrated stress response. *EMBO Rep* 2016;**17**:1374−95.
9. Tabas I. The role of endoplasmic reticulum stress in the progression of atherosclerosis. *Circ Res* 2010;**107**:839−50.
10. Okada K, Minamino T, Tsukamoto Y, Liao YL, Tsukamoto O, Takashima S, et al. Prolonged endoplasmic reticulum stress in hypertrophic and failing heart after aortic constriction—possible contribution of endoplasmic reticulum stress to cardiac myocyte apoptosis. *Circulation* 2004;**110**:705−12.
11. Kassan M, Galan M, Partyka M, Saifudeen Z, Henrion D, Trebak M, et al. Endoplasmic reticulum stress is involved in cardiac damage and vascular endothelial dysfunction in hypertensive mice. *Arterioscler Thromb Vasc Biol* 2012;**32**:1652−61.
12. Noda T, Maeda K, Hayano S, Asai N, Enomoto A, Takahashi M, et al. New endoplasmic reticulum stress regulator, gipie, regulates the survival of vascular smooth muscle cells and the neointima formation after vascular injury. *Arterioscler Thromb Vasc Biol* 2015;**35**:1246−53.
13. Minamino T, Komuro I, Kitakaze M. Endoplasmic reticulum stress as a therapeutic target in cardiovascular disease. *Circ Res* 2010;**107**:1071−82.
14. Di Paola S, Micaroni M, Di Tullio G, Buccione R, Di Girolamo M. PARP16/ARTD15 is a novel endoplasmic-reticulum-associated mono-ADP-ribosyltransferase that interacts with, and modifies karyopherin-beta 1. *PLoS One* 2012;**7**:e37352.
15. Jwa M, Chang P. PARP16 is a tail-anchored endoplasmic reticulum protein required for the PERK- and IRE1alpha-mediated unfolded protein response. *Nat Cell Biol* 2012;**14**:1223−30.
16. Vermeulen M, Mulder KW, Denissov S, Pijnappel WWMP, van Schaik FMA, Varier RA, et al. Selective anchoring of TFIID to nucleosomes by trimethylation of histone H3 lysine 4. *Cell* 2007;**131**:58−69.
17. Hamamoto R, Furukawa Y, Morita M, Iimura Y, Silva FP, Li MH, et al. SMYD3 encodes a histone methyltransferase involved in the proliferation of cancer cells. *Nat Cell Biol* 2004;**6**:731−40.
18. Ren TN, Wang JS, He YM, Xu CL, Wang SZ, Xi T. Effects of SMYD3 over-expression on cell cycle acceleration and cell proliferation in

MDA-MB-231 human breast cancer cells. *Med Oncol* 2011;**28 Suppl 1**:S91−8.
19. Chen YJ, Tsai CH, Wang PY, Teng SC. SMYD3 promotes homologous recombination *via* regulation of H3K4-mediated gene expression. *Sci Rep* 2017;**7**:3842.
20. Mazur PK, Reynoird N, Khatri P, Jansen PW, Wilkinson AW, Liu S, et al. SMYD3 links lysine methylation of MAP3K2 to ras-driven cancer. *Nature* 2014;**510**:283−7.
21. Luo X, Yang D, Wu W, Long F, Xiao C, Qin M, et al. Critical role of histone demethylase Jumonji domain-containing protein 3 in the regulation of neointima formation following vascular injury. *Cardiovasc Res* 2018;**114**:1894−906.
22. Youm YH, Nguyen KY, Grant RW, Goldberg EL, Bodogai M, Kim D, et al. The ketone metabolite beta-hydroxybutyrate blocks NLRP3 inflammasome-mediated inflammatory disease. *Nat Med* 2015;**21**:263−9.
23. Chiong M, Cartes-Saavedra B, Norambuena-Soto I, Mondaca-Ruff D, Morales PE, Garcia-Miguel M, et al. Mitochondrial metabolism and the control of vascular smooth muscle cell proliferation. *Front Cell Dev Biol* 2014;**2**:72.
24. Sang SM, Lambert JD, Ho CT, Yang CS. The chemistry and biotransformation of tea constituents. *Pharmacol Res* 2011;**64**:87−99.
25. Suntar I, Sureda A, Belwal T, Silva AS, Vacca RA, Tewari D, et al. Natural products, PGC-1 alpha, and duchenne muscular dystrophy. *Acta Pharm Sin B* 2020;**10**:734−45.
26. Wang J, Zhu C, Song D, Xia R, Yu W, Dang Y, et al. Epigallocatechin-3-gallate enhances ER stress-induced cancer cell apoptosis by directly targeting PARP16 activity. *Cell Death Dis* 2017;**3**:17034.
27. Kim SY, Kwon YW, Jung IL, Sung JH, Park SG. Tauroursodeoxycholate (TUDCA) inhibits neointimal hyperplasia by suppression of ERK *via* PKCalpha-mediated MKP-1 induction. *Cardiovasc Res* 2011;**92**:307−16.
28. Luo H, Zhou C, Chi J, Pan S, Lin H, Gao F, et al. The role of tauroursodeoxycholic acid on dedifferentiation of vascular smooth muscle cells by modulation of endoplasmic reticulum stress and as an oral drug inhibiting in-stent restenosis. *Cardiovasc Drugs Ther* 2019;**33**:25−33.
29. Hu S, Liu Y, You T, Heath J, Xu L, Zheng X, et al. Vascular semaphorin 7A upregulation by disturbed flow promotes atherosclerosis through endothelial beta 1 integrin. *Arterioscler Thromb Vasc Biol* 2018;**38**:335−43.
30. Moulos P, Sarris ME, Talianidis I. Mechanism of gene-specificity of oncogenic regulators. *Cell Cycle* 2016;**15**:2227−8.
31. Szegezdi E, Logue SE, Gorman AM, Samali A. Mediators of endoplasmic reticulum stress-induced apoptosis. *EMBO Rep* 2006;**7**:880−5.
32. Kawaguchi S, Ng DT. Cell biology. Sensing ER stress. *Science* 2011;**333**:1830−1.
33. Takayanagi T, Kawai T, Forrester SJ, Obama T, Tsuji T, Fukuda Y, et al. Role of epidermal growth factor receptor and endoplasmic reticulum stress in vascular remodeling induced by angiotensin II. *Hypertension* 2015;**65**:1349−55.
34. Ishimura S, Furuhashi M, Mita T, Fuseya T, Watanabe Y, Hoshina K, et al. Reduction of endoplasmic reticulum stress inhibits neointima formation after vascular injury. *Sci Rep* 2014;**4**:6943.
35. Park SW, Ozcan U. Potential for therapeutic manipulation of the UPR in disease. *Semin Immunopathol* 2013;**35**:351−73.
36. Di Girolamo M. Regulation of nucleocytoplasmic transport by ADP-ribosylation: the emerging role of karyopherin-beta 1 mono-ADP-ribosylation by ARTD15. *Curr Top Microbiol Immunol* 2015;**384**:189−209.
37. Wen Y, Zhao R, Gupta P, Fan Y, Zhang Y, Huang Z, et al. The epigallocatechin gallate derivative Y6 reverses drug resistance mediated by the ABCB1 transporter both *in vitro* and *in vivo*. *Acta Pharm Sin B* 2019;**9**:316−23.
38. Zhu Y, Zhu MX, Zhang XD, Xu XE, Wu ZY, Liao LD, et al. SMYD3 stimulates EZR and LOXL2 transcription to enhance proliferation, migration, and invasion in esophageal squamous cell carcinoma. *Hum Pathol* 2016;**52**:153−63.
39. Wang L, Wang QT, Liu YP, Dong QQ, Hu HJ, Miao Z, et al. ATM signaling pathway is implicated in the SMYD3-mediated proliferation and migration of gastric cancer cells. *J Gastric Cancer* 2017;**17**:295−305.
40. Kim JM, Kim K, Schmidt T, Punj V, Tucker H, Rice JC, et al. Cooperation between SMYD3 and PC4 drives a distinct transcriptional program in cancer cells. *Nucleic Acids Res* 2015;**43**:8868−83.
41. Proserpio V, Fittipaldi R, Ryall JG, Sartorelli V, Caretti G. The methyltransferase SMYD3 mediates the recruitment of transcriptional cofactors at the myostatin and c-Met genes and regulates skeletal muscle atrophy. *Genes Dev* 2013;**27**:1299−312.